1-1-2017

Acute Temporal Changes of MRI-Tracked Tumor Vascular Parameters after Combined Anti-angiogenic and Radiation Treatments in a Rat Glioma Model: Identifying Signatures of Synergism.

Rasha Elmghirbi
Henry Ford Health System

Tavarekere N. Nagaraja
Henry Ford Health System, TNagara1@hfhs.org

Stephen L. Brown
Henry Ford Health System, Sbrown1@hfhs.org

Swayamprava Panda
Henry Ford Health System

Madhava P. Aryal

See next page for additional authors

Recommended Citation

Elmghirbi R, Nagaraja TN, Brown SL, Panda S, Aryal MP, Keenan KA, Bagher-Ebadian H, Cabral G, and Ewing JR. Acute temporal changes of mri-tracked tumor vascular parameters after combined anti-angiogenic and radiation treatments in a rat glioma model: Identifying signatures of synergism. Radiat Res 2017; 187(1):79-88.

Authors

Rasha Elmghirbi, Tavarekere N. Nagaraja, Stephen L. Brown, Swayamprava Panda, Madhava P. Aryal, Kelly A. Keenan, Hassan Bagher-Ebadian, Glauber Cabral, and James R. Ewing

RADIATION RESEARCH **187**, 79–88 (2017)
0033-7587/17 $15.00

DOI: 10.1667/RR14358.1

Acute Temporal Changes of MRI-Tracked Tumor Vascular Parameters after Combined Anti-angiogenic and Radiation Treatments in a Rat Glioma Model: Identifying Signatures of Synergism

Rasha Elmghirbi,[a,b] Tavarekere N. Nagaraja,[c] Stephen L. Brown,[d,1] Swayamprava Panda,[b] Madhava P. Aryal,[e] Kelly A. Keenan,[c] Hassan Bagher-Ebadian,[a,d] Glauber Cabral[b] and James R. Ewing[a,b,f]

[a] *Department of Physics, Oakland University, Rochester, Michigan; Departments of* [b] *Neurology,* [c] *Neurosurgery and* [d] *Radiation Oncology, Henry Ford Hospital, Detroit, Michigan;* [e] *Department of Radiation Oncology, University of Michigan Medical School, Ann Arbor, Michigan; and* [f] *Department of Neurology, Wayne State University, Detroit, Michigan*

Elmghirbi, R., Nagaraja, T. N., Brown, S. L., Panda, S., Aryal, M. P., Keenan, K. A., Bagher-Ebadian, H., Cabral, G. and Ewing J. R. Acute Temporal Changes of MRI-Tracked Tumor Vascular Parameters after Combined Anti-angiogenic and Radiation Treatments in a Rat Glioma Model: Identifying Signatures of Synergism. *Radiat. Res.* 187, 79–88 (2017).

In this study we used magnetic resonance imaging (MRI) biomarkers to monitor the acute temporal changes in tumor vascular physiology with the aim of identifying the vascular signatures that predict response to combined anti-angiogenic and radiation treatments. Forty-three athymic rats implanted with orthotopic U-251 glioma cells were studied for approximately 21 days after implantation. Two MRI studies were performed on each animal, pre- and post-treatment, to measure tumor vascular parameters. Two animal groups received treatment comprised of Cilengitide, an anti-angiogenic agent and radiation. The first group received a subcurative regimen of Cilengitide 1 h before irradiation, while the second group received a curative regimen of Cilengitide 8 h before irradiation. Cilengitide was given as a single dose (4 mg/kg; intraperitoneal) after the pretreatment MRI study and before receiving a 20 Gy radiation dose. After irradiation, the post-treatment MRI study was performed at selected time points: 2, 4, 8 and 12 h ($n = \geq 5$ per time point). Significant changes in vascular parameters were observed at early time points after combined treatments in both treatment groups (1 and 8 h). The temporal changes in vascular parameters in the first group (treated 1 h before exposure) resembled a previously reported pattern associated with radiation exposure alone. Conversely, in the second group (treated 8 h before exposure), all vascular parameters showed an initial response at 2–4 h postirradiation, followed by an apparent lack of response at later time points. The signature time point to define the "synergy" of Cilengitide and radiation was 4 h postirradiation. For example, 4 h after combined treatments using a 1 h separation (which followed the subcurative regimen), tumor blood flow was significantly decreased, nearly 50% below baseline ($P = 0.007$), whereas 4 h after combined treatments using an 8 h separation (which followed the curative regimen), tumor blood flow was only 10% less than baseline. Comparison between the first and second groups further revealed that most other vascular parameters were maximally different 4 h after combined treatments. In conclusion, the data are consistent with the assertion that the delivery of radiation at the vascular normalization time window of Cilengitide improves radiation treatment outcome. The different vascular responses after the different delivery times of combined treatments in light of the known tumor responses under similar conditions would indicate that timing has a crucial influence on treatment outcome and long-term survival. Tracking acute changes in tumor physiology after monotherapy or combined treatments appears to aid in identifying the beneficial timing for administration, and perhaps has predictive value. Therefore, judicial timing of treatments may result in optimal treatment response.

INTRODUCTION

Glioblastoma (GBM) remains one of the most lethal cancers, with a 15-month average overall survival (OS), even with optimal treatment (*1*). The combination of therapies are more effective than a monotherapy in treating GBM and improving patient OS and quality of life (*2, 3*). In preclinical studies, the optimum short-term order and timing of combined treatments can significantly influence OS (*4–6*). Since these potential ''synergies'' are short-term with respect to tumor response, and many of the agents affect tumor vasculature, it might be expected that the short-term changes in tumor physiology which occur in response to combined treatments could be used as biomarkers of response. Indeed, studies in preclinical models (*7, 8*) showed that tumor physiology changes profoundly in the hours after either anti-angiogenic treatment or irradiation. In current clinical practice, short-term anatomical changes don't occur and short-term physiological responses are not

[1] Address for correspondence: Henry Ford Hospital, Department of Radiation Oncology, 2799 West Grand Blvd. Detroit, MI 48202-2689; email: sbrown1@hfhs.org.

usually assessed. Instead, a delayed assessment (weeks or months later) based on tumor volume, e.g., the response evaluation criteria in solid tumors (RECIST) (*9, 10*), or more recently, revised assessment in neuro-oncology (RANO) (*11, 12*) criteria, is used to evaluate responses.

Cilengitide is an anti-angiogenic agent which, when combined with radiation in preclinical studies, has been shown to increase OS compared to radiation treatment alone (*4*). It has multimodal anti-glioma effects such as cytotoxic, anti-angiogenic, anti-invasive and synergistic effects (*13*). Mikkelsen *et al.* (*4*) reported that a single injection of Cilengitide given 4–12 h before irradiation had a therapeutic benefit when combined with radiation in a U-251 cerebral glioma model. However, when Cilengitide was administered outside that time window, it showed little additional effect on OS. Nagaraja *et al.* observed short-term effects of Cilengitide on the tumor vasculature of U-251 cerebral glioma in athymic rats, demonstrating that it exerted a short-term effect on transvascular transfer parameters of the tumor vasculature, causing vascular normalization at approximately 8 h after treatment (*7*). It has been suggested that normalization of the vasculature increased radiosensitivity and enhanced treatment efficacy (*14*).

The importance of optimizing the timing and sequence of combined therapies such as radiotherapy with anti-angiogenic drugs has become increasingly recognized (*15–18*), as has the importance of acute tumor responses to therapies (*4, 5, 7, 8, 19*). In this study, we investigated the timing between Cilengitide and radiation exposure to determine the vascular signature corresponding to increased tumor response to combined treatments. Dynamic contrast-enhanced magnetic resonance imaging (DCE-MRI) with model selection (*20–22*) along with Patlak *et al.* (*23, 24*) and Logan *et al.* (*25, 26*) graphical methods were used to measure tumor vascular parameters in a U-251 rat model of embedded cerebral tumor. Based on the duration of time between Cilengitide treatment and radiation exposure, the effects on tumor vascular physiology were evaluated in two groups, one associated with a sub-curative response (drug given 1 h before irradiation), and one associated with a curative response (drug given 8 h before irradiation). Acute changes in tumor vascular parameters were monitored in the hours after the combined treatments to detect responses.

MATERIALS AND METHODS

These studies were approved by the Henry Ford Hospital Institutional Animal Care and Use Committee (IACUC). Forty-three athymic rats were intracerebrally inoculated with U-251 tumor cells. Approximately three weeks after implantation, two MRI studies were performed 24 h apart for each animal, with MRI vascular parameters measured in the two sessions. Animals were exposed to radiation as the second part of the combined treatments at 2, 4, 8 or 12 h before the second MRI. Immediately after the second MRI session, the brain of the anesthetized animal was removed for histology.

The U-251 Orthotopic Brain Tumor Model

Athymic nude rats (n = 43) (~8 weeks old; Charles River Laboratories, Wilmington, MA) were implanted intracerebrally with U-251 MG tumor cells. Animals were anesthetized with isoflurane (4% for induction, 0.75–1.5% for maintenance, balance N_2O:O_2 = 2:1). The surgical zone was swabbed with Betadine® solution, the eyes coated with Lacri-Lube® and the head immobilized in a small animal stereotactic device (Kopf® Instruments, Tujunga, CA). After draping, a 1 cm incision was made 2 mm to the right of the midline and the skull was exposed. A burr hole was drilled 3.5 mm to the right of bregma, taking care not to penetrate the dura mater. A 10 μl Hamilton syringe with a 26g needle (model no. 701, Hamilton Co., Reno, NV) containing U-251 MG tumor cells freshly harvested from log phase growth (5×10^5 in 10 μl of PBS) was lowered to a depth of 3.0 mm and then raised back to a depth of 2.5 mm to create a pocket. Cells were injected at a rate of 0.5 μl/10 s until the entire volume was injected. The syringe was then slowly withdrawn, the burr hole sealed with sterile bone wax and the skin sutured. Tumors in animals implanted following this technique grew to 3–5 mm diameter in approximately 3 weeks after implantation.

Between day 18 and 21 after implantation, two MRI studies were performed 24 h apart for each animal. Animals were anesthetized with isoflurane (4% for induction, 0.75–1.5% for maintenance, balance N_2O:O_2 = 2:1) and allowed to spontaneously respire. A tail vein was cannulated for the administration of the contrast agent. Body temperature was maintained constant (37°C) with a warm air supply monitored via an intrarectal type T thermocouple.

Treatment Protocol

Animals were divided into two groups, all animals received Cilengitide and radiation treatments, the two groups were distinguished by the interval between administration of Cilengitide and time of exposure to radiation.

Animals were exposed to radiation, at 1 (n = 21) and 8 h (n = 22), after Cilengitide treatment. Each group was further divided into four subgroups (n = 5 or 6 per subgroup) according to the time point of irradiation (2, 4, 8 and 12 h) preceding the second MRI. Thus, the entire timeline of the studies falls within the 24 h time interval between the two MRI studies. Figure 1 shows the timing of combined treatments and MRIs for each group.

Cilengitide Administration

A single 4 mg/kg dose (i.p.) of Cilengitide was administered after the pretreatment MRI study at 1 and 8 h preirradiation. Normal saline was the diluent and the injected volume was 0.2 ml. Cilengitide was purchased commercially from Selleck Chemicals (Houston, TX).

Radiation Treatment

The protocol for radiation treatment is described in detail in Brown *et al.* (*8*). Briefly, radiation was delivered using a clinical linear accelerator operating at 6 MV photons (Varian Trilogy, Palo Alto, CA). The location of the tumor was determined from the pretreatment MRI study, and referenced to the burr hole used to implant the tumor. After anesthesia (80 mg/kg ketamine and 8 mg/kg xylazine), rats were placed in a stereotactic device with the rat head in the same orientation as when tumor cells were implanted. A total dose of 20 Gy was delivered at an approximate dose rate of 8 Gy/min using 8 × 8 cm primary collimation, a 6 mm diameter cone as a secondary collimator, a source-to-surface distance of 75 cm, a 14 mm bolus above the skull for electron equilibrium at the tumor depth and a linear accelerator output rate set at 800 monitor units per min. The tumor dimensions were covered by the 100% isodose line. The treatment beam projected in a single anterior-posterior direction from the top of the skull through the tumor on the right hemisphere exiting under the jaw.

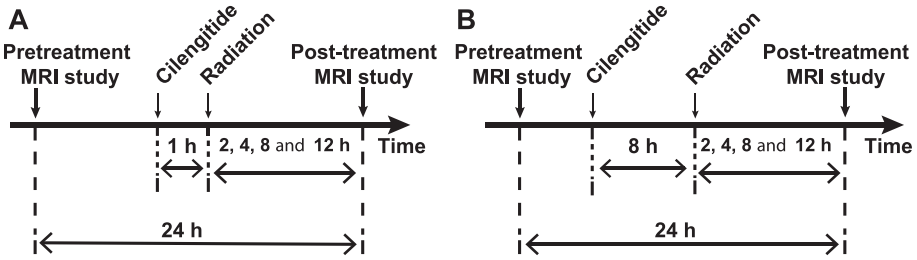

FIG. 1. Experiment timeline. Cilengitide was administrated 1 h (panel A) or 8 h (panel B) prior to irradiation. In both groups, post-treatment MRIs were performed at 2, 4, 8 or 12 h postirradiation. Of note, the time between the two MRIs was consistently 24 h.

MRI Studies

All studies were performed using a Varian 7-Tesla MRI magnet (Santa Clara, CA) 20 cm bore system with a DirectDrive spectrometer and console. Gradient maximum strengths and rise times were 250 mT/m and 120 μs. All MRI image sets were acquired with a 32×32 mm^2 field of view. The transmit coil was a Bruker-supplied volume resonator and the receive coil was a Bruker 2 cm surface coil for rat brain imaging (Billerica, MA). Arterial spin labeling (ASL), DCE-MRI, Look-Locker (LL), T_1-weighted and diffusion weighted imaging (DWI) acquisitions were used to describe the state of the vasculature after treatment.

Spin-echo arterial spin-labeled data were acquired to estimate cerebral blood flow in a single central slice, as previously described elsewhere (*27*). Sets of MRI parameters were obtained with alternating gradients and frequency offsets in combinations of four, as follows: matrix = 128 × 64, one 1.0 mm slice, NA = 2, TE/TR = 24/1500. Arterial labeling = 1 s. Total time = 13 min.

The DCE-MRI sequence was a dual-echo gradient-echo (2GE) sequence, the ''mgems'' sequence in the Agilent VnmrJ library. The 2GE sequence acquired a set of three slices on 2 mm centers (1.8 mm slice, 0.2 mm gap). The slice set was centered on the tumor and 150 image sets at 4.0 s intervals were acquired with the following parameters: flip angle (FA) = 25°, matrix = 128 × 64, NE = 2, NA = 1, TE1/TE2/TR = 2.0/4.0/60 ms. Total run time was 10 min. At image 15 of the 2GE sequence, a bolus injection of the contrast agent (Magnevist®; Bayer HealthCare LLC, Wayne, NJ), 0.25 mmol/kg at undiluted concentration, no flush, was performed by hand push, followed by a slight draw-back. The purpose of the draw-back was to equilibrate intravascular pressure and to allow confirmation that blood was in the line and the injection was delivered intravascularly. Prior to the DCE-MRI sequence, and immediately after, two LL sequences were run so that a voxel-by-voxel estimate of longitudinal relaxation time (T_1) in the tissue could be made pre- and post-contrast agent administration. LL sequence parameters were as follows: FA = 15°, matrix 128 × 64, five 2.0 mm slices, no gap. NE = 24 inversion-recovery echoes on 50 ms intervals, TE/TR = 4.0 ms/2,000 ms.

Prior to the pre-contrast LL sequence, and after the post-contrast LL sequence, two high-resolution T_1-weighted spin-echo images were acquired before and after administration of the contrast agent with the following parameters: FA = 45°, 180°, matrix 256 × 192, 27 slices, 0.4 mm thickness, 0.1 mm gap, NE = 1, NA = 4, TE/TR = 16 ms/800 ms. After the post-contrast LL sequence, a pulsed-gradient spin-echo DWI sequence was run in three directions (x, y, z) to generate a parametric map of apparent diffusion coefficient (ADC). DWI sequence parameters were as follows: matrix 128 × 64, 13 slices, 0.8 mm thickness, 0.2 mm gap, TR = 1,500 ms, TE = 40 ms, NE = 1, b-values = 0, 600, 1,217 s/mm^2, gradient amplitude = 107 mT/m, gradient duration = 10 ms.

Tumor Vascular Parameters

The MRI vascular parameters were estimated using the following: 1. ASL for estimating tumor blood flow (TBF) (*27, 28*); 2. Patlak *et al*., extended Patlak and Blasberg (*23, 24*) [identical to extended Tofts *et al*. (*31*)] and Logan *et al*. analyses (*25, 29, 30*) of DCE-MRI data, using a model-selection paradigm (*20–22*) to estimate the plasma volume fraction (v_p), forward volumetric transfer constant (K^{trans}), interstitial volume fraction (v_e) and extracellular volume fraction (V_D); and 3. DWI to estimate ADC. As previously noted elsewhere (*30*), the extracellular volume fraction, V_D, can be estimated using Logan plots; herein, V_D will be used as a biomarker of treatment response. V_D has been shown to correlate with tumor cellular density ($r = -0.75$, $P < 0.001$), and to strongly correlate with the extended Tofts model (*31*) estimate of $v_p + v_e$ ($r = 0.91$, $P < 0.001$). However, it will become clear that V_D is a more stable estimate of extracellular volume than is the sum $v_p + v_e$.

Model selection generates maps of brain regions and labels them with the number of parameters used to describe the data. This results in regions that map: 1. Only plasma volume, v_p (essentially normal vasculature with no leakage, where the filling of the vasculature with contrast agent in the plasma occurs), named as the model 1 region; 2. v_p and K^{trans} (tissue regions with leakage, but with only blood-to-brain influx,), named as the model 2 region; or 3. v_p, K^{trans} and v_e (highly leaky vessels with measurable reflux of contrast agent from the interstitial space to the microvasculature), named as the model 3 region. Quantitative maps of MRI vascular parameters were generated for pre- and post-treatment imaging sessions. The MRI slice with the largest tumor cross-section was selected and the model 3 region of interest (ROI) was used to define the extent of the tumor.

The advantage of using a model selection paradigm is that the border between tumor and surrounding normal tissue can be well defined by the changing permeability of the tissue, with the tumor tissue typically permeable to a contrast agent, and the normal tissue typically impermeable across the time of the 9 min study. In all animals, post-contrast T_1-weighted images and hematoxylin and eosin (H&E)-stained sections were used to confirm the tumor ROI that was defined by model selection. Figure 2 shows that the tumor boundary on both H&E-stained and post-contrast T_1-weighted images agreed with the tumor boundary defined by the model 3 region.

Histology

After the second MRI study, the animals were continued on isoflurane anesthesia and transcardially perfused with normal saline followed by the fixative, 4% paraformaldehyde. After the brains were carefully removed from the skull, they were stored overnight in the fixative. Coronal slices (2 mm thick) through the tumor were obtained using a rat-brain matrix (Activational Systems Inc., Warren, MI). The brain tissue was processed using a Tissue-Tek® VIP processor and embedded in paraffin. Sections (7 μm thick) were cut from the paraffin block corresponding to the MRI slice and placed on Superfrost Plus (Fisher Scientific, Pittsburgh, PA) slides. It contained the largest tumor area and was H&E stained for evaluation of tumor ROIs. Images were collected using a Nikon® Eclipse E800 microscope equipped with ACT1C software. A comparative ROI was chosen within the contralateral hemisphere, usually within the caudate putamen. Both

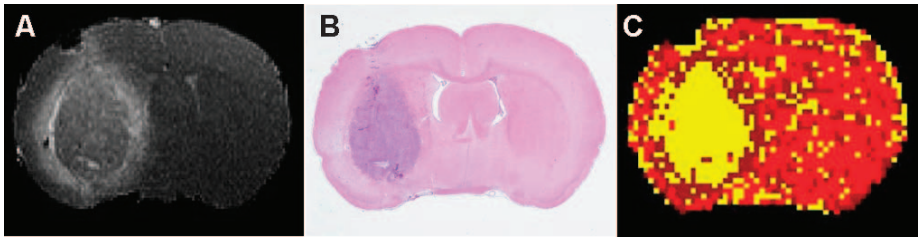

FIG. 2. Panel A: High-resolution post-contrast agent T_1-weighted image. Panel B: H&E staining of a centrally located tissue slice approximately corresponding to the central slice of the MRI study. Panel C: Model selection map. Yellow indicates model 3 acceptance (regions associated with highly leaky vasculature along with backflux), dark red indicates model 2 acceptance (bordered model 3 regions, showing leakage at reduced rates) and red indicates model 1 acceptance (normal nonleaky brain tissue). Note the anatomical agreement in the position and distribution of the tumor mass and boundary between the model 3 region, T_1 MRI and H&E images. The rat brain is approximately 1.5 cm across (transverse direction).

1× low magnification of the entire coronal section and 10× high magnification images were collected. Images were imported into ImageJ version 1.43u (NIH, Bethesda, MD) and converted to 8 bits for analysis.

Statistical Analysis

All MRI vascular parameters were measured in the model 3 ROI and are reported as mean ± standard error of the mean (SEM) for both pre- and post-treatment MRI sessions. Vascular measurements at the time points after treatment were compared with pretreatment values for the same rats.

To make the effect of an intervention easily understood, pre- and post-treatment differences were computed as percentage changes. To avoid bias, the percentage change was calculated as $\{(\text{post} - \text{pre})/[2 \times (\text{mean of post} + \text{pre})]\}\%$ for each parameter, allowing a maximum change of ±100%, but preserving the assumption that the two samples (pre and post) were drawn from the same population. Dividing the difference by the mean generates an unbiased estimator of change because the sources of error in the numerator and denominator are balanced. In contrast, the percentage change calculated as [(post – pre)/(pre)]% is a biased estimator and strongly influenced by the baseline value, since it has two sources of error in numerator and one in denominator (*32*). In addition, Shapiro-Wilk tests were performed to test normality in the percentage change data computed by both methods for the 1 and 8 h groups. The null hypothesis was that if the P value was >0.1, then the sample is more likely to be normally distributed.

A paired t test was applied for all vascular parameters to determine significances in the percentage change for each time point in the 1 and 8 h groups: at 2, 4, 8 and 12 h. Additionally, percentage differences between the 1 and 8 h groups at 4 h postirradiation were tested using an unpaired Student's t test. Differences in $P < 0.05$ were considered statistically significant. To illustrate the treatment responses in the 1 and 8 h groups, the mean percentage change at each time point was plotted against time for all vascular parameters. Error bars on the graphs represent the standard error of the mean percentage change for each time point.

RESULTS

The temporal variation of tumor physiology in the two groups (Cilengitide administered either 1 or 8 h before irradiation) was studied by MRI at 2, 4, 8 and 12 h postirradiation. An example of the parametric maps of model selection, DCE-MRI vascular parameters K^{trans} and v_e, TBF and ADC are shown in Fig. 3. Figure 3A and B show representative pre- and post-treatment parametric maps for animals selected from the 1 and 8 h treatment groups, MRI studies performed at 4 h postirradiation.

The mean of the ASL-estimated tumor blood flow in the ROIs of the pretreatment population of 43 animal studies was 113.2 ± 5.8 [ml/100 ml-min]. The DCE-MRI vascular parameters in tumor prior to treatment were: $K^{trans} = (4.74 \pm 0.25) \times 10^{-2}$ [min^{-1}]; $v_e = 15.51 \pm 0.60\%$; $V_D = 16.88 \pm 0.63\%$. The pretreatment ADC value was $(2.52 \pm 0.07) \times 10^{-3}$ [mm^2/s]. Pretreatment values for all parameters across animals were normally distributed.

As noted, to avoid bias the percentage change in parametric estimates was calculated as $\{(\text{post} - \text{pre})/[2 \times (\text{mean of post} + \text{pre})]\}\%$ instead of [(post – pre)/(pre)]% (*32*). When the two methods were applied to our data and compared, the latter method produced significantly non-normally distributed data sets in two vascular parameters, and it produced more skewed data in most vascular parameters, as shown in Table 1.

Figure 4 shows the percentage change as a function of time for the vascular parameters, TBF, K^{trans}, v_e, V_D and ADC, in the model 3 region, i.e., the tumor region of interest, for 1 and 8 h treatment groups. Significant changes in vascular parameters were observed at early hours in the 1 and 8 h treatment groups after the combination of Cilengitide and radiation exposure.

In the 1 h group (Fig. 4A), TBF showed a significant decrease of about 40 ± 5% below the pretreatment levels at 2 h postirradiation ($P = 0.001$), and continued to decline to 50 ± 10% at 4 h postirradiation ($P = 0.007$). Subsequently, TBF increased markedly to pretreatment values at 8 and 12 h postirradiation, to the extent that the average TBF values were not significantly different from pretreatment levels ($P > 0.10$). Conversely, K^{trans} increased above the pretreatment values, reaching its maximum value of around 15 ± 3% at 4 and 8 h, and then sharply declined to 10 ± 4% below the pretreatment level at 12 h postirradiation. K^{trans} values significantly increased above pretreatment values at 4 ($P = 0.034$) and 8 h ($P = 0.003$) postirradiation. The temporal profile of v_e resembled that of K^{trans}; except that v_e values were much closer to the pretreatment levels and then

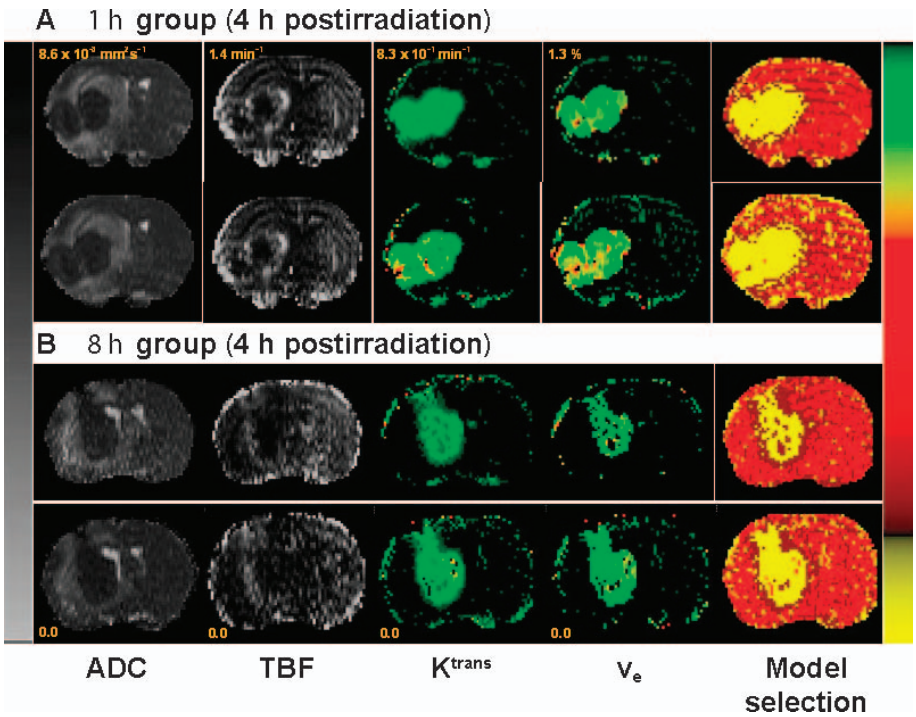

FIG. 3. Representative sets of pre- and post-treatment parametric maps from the 1 (panel A) and 8 h (panel B) groups at 4 h postirradiation. Maps from left to right: ADC, TBF, K^{trans}, v_e and model selection; pretreatment is shown in the top row and post-treatment in the bottom row. The left scale bar is shared between ADC and TBF maps for both sets, but has different scaling as indicated in the range for each. The right color scale bar is given in common to K^{trans}, v_e and model selection maps, but also with different scaling for each parameter. For the model selection map, yellow is model 3 acceptance, dark red is model 2 acceptance and red is model 1 acceptance. Note the improvement in TBF in the post-treatment map for the 8 h group and the lack of change between pre- and post-treatment in K^{trans} maps, which indicate vascular normalization and evidence of treatment effect at this time point.

reduced to 8 ± 3% below pretreatment value at 12 h postirradiation. There was no significant change throughout the study in v_e values before and after treatment. V_D started below pretreatment levels at 2 and 4 h, followed by an increase to the pretreatment value at 8 h postirradiation, and then a significant decline to 10 ± 3% below pretreatment level at 12 h postirradiation ($P = 0.033$). It appears that V_D and TBF changed together, up to 12 h postirradiation.

A marked difference in the pattern of vascular responses between the two groups was apparent starting at 4 h postirradiation. In the 8 h group (Fig. 4B), TBF at 2 h postirradiation significantly decreased by about 33 ± 10%

TABLE 1
Normality Test and Skewness for the Two Methods of Percentage Change in 1 and 8 h Groups for all MRI Vascular Parameters

	Shapiro-Wilk normality test (*P* value)		Skewness	
	[(post − pre)/2×(mean of post + pre)]%	[(post − pre)/(pre)]%	[(post − pre)/2×(mean of post + pre)]%	[(post − pre)/(pre)]%
1 h group				
TBF	0.451	0.118	0.091	0.716
K^{trans}	0.130	0.324	−0.650	−0.273
v_e	0.849	0.446	0.103	0.540
V_D	0.998	0.900	0.001	0.485
ADC	0.568	0.209	0.585	0.863
8 h group				
TBF	0.762	0.083*	−0.185	1.116**
K^{trans}	0.210	0.070*	0.157	0.545
v_e	0.964	0.591	0.045	0.589
V_D	0.469	0.729	−0.338	0.011
ADC	0.406	0.526	−0.358	−0.220

* Not normally distributed ($P < 0.10$).
** Significantly skewed.

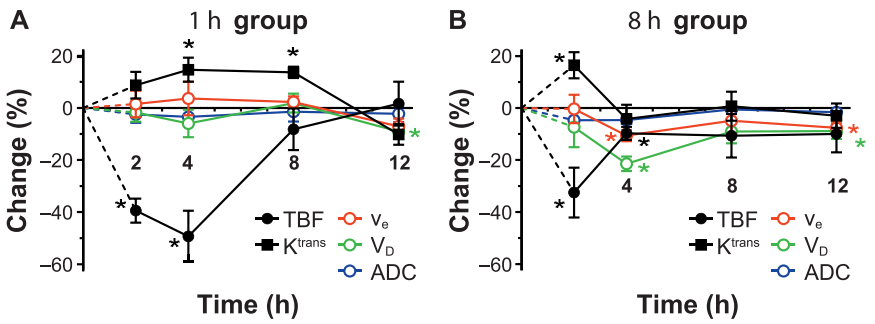

FIG. 4. Percentage change versus time in the MRI vascular parameters after combined Cilengitide and radiation treatments in the tumor region of interest. Cilengitide was administered 1 (panel A) or 8 h (panel B) before irradiation. The pattern of response in the 1 h group resembles that of irradiation alone [see fig. 2 in ref. (*7*)], while the pattern of response in the 8 h group shows a preservation of the vascular parameters starting at 4 h postirradiation and indicates a synergistic effect. $*P < 0.05$.

from pretreatment levels ($P = 0.043$), followed by an increase to near pretreatment values at 4 h postirradiation ($P = 0.031$). Afterward, TBF values remained near pretreatment values. In contrast, K^{trans} was elevated to 18 ± 5% over pretreatment values at 2 h postirradiation ($P = 0.047$), and then declined to near pretreatment levels at 4 h postirradiation and beyond. Similarly, v_e and V_D values started slightly below pretreatment levels at 2 h postirradiation and then significantly decreased at 4 h postirradiation to 10 ± 2% ($P = 0.008$) and 23 ± 3% ($P = 0.001$) below pretreatment values. Afterward, v_e and V_D returned to 5 ± 2% ($P = 0.030$) and 10 ± 3% ($P = 0.036$) below pretreatment levels at 12 h postirradiation.

ADC was estimated in the 1 h and 8 h groups and showed no change throughout the study (Fig. 4A and 4B). The associated error bars were large and the trends were unremarkable over the experiment period.

DISCUSSION

In clinical oncology, the timing of chemotherapy, including antiangiogenic agents that affect tumor vasculature, is seldom considered in relationship to the time of radiotherapy. However, as the results of this investigation indicate, timing can be critical to the resulting tumor physiology, and consequently to tumor response. Identifying the characteristic changes in tumor physiology after combined treatments that optimize tumor response may lead to synergies in treatment efficacy, and to significant improvements in the control of solid tumors.

Published preclinical studies have shown that the sequence and timing of anti-angiogenic drug and radiation administration affects therapeutic outcome and OS (*15–18*). Timing-dependent outcomes appear to be related to acute changes in the tumor vascular physiology in the hours after a monotreatment or combined treatments (*4, 5, 7, 8, 19*). Furthermore, by tracking short-term changes in tumor vascular physiology, a beneficial timing of the combined therapies can be identified, leading to better treatment outcome and OS.

In previously published work, DCE-MRI parameters have been shown to be reliable early biomarkers of tumor response to treatment (*33–35*); they can characterize tissue vasculature and are sensitive to vascular changes related to tumor angiogenesis. Here, an ASL estimate of TBF and DCE-MRI estimates of K^{trans}, v_e and V_D were used to evaluate the temporal characteristics of the acute therapeutic tumor response. Since each one of these parameters gives insight into a separate physiological factor, examination of the spectrum of MRI tumor biomarkers and changes in their relationship to one another can illuminate the physiology of a therapeutic response.

In this study, we chose two intervals between Cilengitide treatment and irradiation, and attempted to identify acute temporal changes in tumor vascular parameters in a U-251 cerebral glioma rat model. Our choice of the intervals between Cilengitide treatment and irradiation was based on a knowledge of the temporal profile of acute changes in the tumor vascular parameters after Cilengitide treatment alone reported by Nagaraja *et al.* (*7*), and of irradiation alone reported by Brown *et al.* (*8*). Nagaraja and colleagues tracked the short-term changes in the tumor vascular parameters (K^{trans} and v_e) at 2, 4, 8, 12 and 24 h after Cilengitide administration in an orthotopic U-251 glioma model. They found that vascular parameters pivoted around the 8 h time point, with 2 and 4 h groups showing increases, 12 and 24 h groups showing decreases and values at 8 h being close to the pretreatment baseline values, indicating that Cilengitide caused vascular normalization at 8 h after treatment. This vascular normalization coincided with a previously published study (*4*) in which increased treatment efficacy and OS were reported when Cilengitide was given within 4–12 h prior to irradiation. In support of this finding, it was reported in a mouse model with a human GBM (*36*) that the outcome of radiation treatment was superior when administered during the time window of normalization. We concluded that pharmacological ''normalization'' of vasculature (*14*) had the potential to increase sensitivity to radiation.

Acute changes in tumor vascular parameters hours after exposure to a single 20 Gy radiation dose in an orthotopic U-251 brain tumor model were investigated by Brown *et al.* (*8*). The parameters, TBF, K^{trans} and v_e were measured at 2, 4, 8, 12 and 24 h after irradiation and the temporal changes were recorded; significant changes in all vascular parameters were observed in the hours after the 20 Gy irradiation. Since no synergy would be expected in the 1 h group, the temporal profile of tumor vascular parameters would be expected to be similar to that of irradiation alone. In addition, a therapeutic benefit would be expected in the 8 h group, and therefore, the temporal pattern of response should be expected to reveal a signature of ''synergy'' in Cilengitide and irradiation.

In the 1 h group (Fig. 4A), the pattern of the temporal changes of tumor vascular parameters followed the same trend as seen previously with irradiation alone, an initial decrease in blood flow followed by a normalization of blood flow at 8 h (*8*), whereas in the 8 h group (Fig. 4B), the temporal changes in tumor vascular parameters showed a much different pattern than in the 1 h group, and appear to serve as a marker of the response to combined Cilengitide and irradiation.

It is to be expected that, after exposure to a large dose of radiation, a transient increase in the vascular permeability will occur, associated with damage to tumor vasculature (*37*). In the 8 h group, K^{trans} was significantly elevated 2 h postirradiation, but, unlike irradiation alone or in the 1 h group, this was then followed by a sharp decline below the pretreatment level at 4 h postirradiation, after which point it remained essentially unchanged. A steep decrease in K^{trans} appears to be evidence of combined drug and radiation treatment effect on tumor vasculature (*35*), probably associated with normalization of the vasculature (*38, 39*). The decrease in K^{trans} was coincident with a significant increase in TBF from 33–10% below pretreatment levels. This observation was in agreement with another published study (*40*), in which it was reported that vascular normalization led to increased tumor perfusion and lower tumor interstitial pressure. Vascular normalization and an increase in tumor perfusion were associated with the increase in OS (*41*). We suggest that irradiation 8 h after the administration of Cilengitide decreases tumor vascular permeability, leading to normalization of the vasculature and improved tumor perfusion. The ''lack'' of response (i.e., resetting and continuation) at 4 h postirradiation indicates that vascular normalization and tumor perfusion were maintained.

On the other hand, v_e and V_D were below pretreatment values throughout the study; their significant reductions of 10 and 23%, respectively, were at 4 h postirradiation. At a later point, v_e and V_D values slightly increased and then remained unchanged. The remarkable decrease in v_e and V_D at 4 h indicates a loss of extracellular space, suggesting that cellular swelling may occur in tumor cells after Cilengitide and high-dose radiation treatment. As previously reported, cellular swelling may be a sign of tumor cell apoptosis (*8, 42*). Lomonaco *et al.* (*19*) found that within hours, treatment with Cilengitide or radiation alone induced autophagy in glioma cells; pretreatment of glioma cells with Cilengitide prior to irradiation resulted in a larger increase in autophagy followed by cell apoptosis and more significant increase in cell death. It appears that Cilengitide sensitizes tumor cells to radiation when radiation is administrated at the vascular normalization time, thus causing tumor cell swelling, which may either induce or signal tumor cell apoptosis. Unlike the 1 h group, the sizeable decrease in v_e and V_D and then the lack of response in later time points serve as a signature of the beneficial timing of Cilengitide and irradiation.

Apparent diffusion coefficient did not show any change in either the 1 or 8 h group throughout the experiment period . It demonstrated a lack of sensitivity to the acute tumor responses hours after Cilengitide and irradiation. In a previously published study, the sensitivity of ADC as a biomarker was explored acutely after anti-angiogenic treatment in a U87 orthotopic mouse glioma model. Only very small changes in ADC were observed 2–3 days after treatment, and ADC was found not to be a sensitive biomarker to anti-VEGF therapy (*35*).

At 4 h postirradiation, K^{trans}, TBF, v_e and V_D showed a lack of response and maintained their values near pretreatment levels. Consequently, we hypothesized that 4 h postirradiation was the signature time point of a beneficial response. The difference between the 1 and 8 h groups at 4 h postirradiation is noteworthy; here, the significant changes occur and differentiate the responses between the two groups (Fig. 5). At 2 h postirradiation, all vascular parameters for the 1 and 8 h groups are similar, whereas at 4 h postirradiation, the vascular parameter values diverge. Specifically, when the 1 and 8 h groups are compared, TBF, K^{trans} and V_D values were significantly different 4 h postirradiation ($P = 0.010$, 0.030 and 0.032, respectively).

It appears that at 4 h postirradiation the combined treatments has a superior therapeutic effect on the tumor cells, and that this effect remained at later time points. Our assumption, supported by the data, is that tumor vasculature and cells are most vulnerable at 4–12 h postirradiation. Therefore, in the event that other therapeutic agents are intended to be delivered in conjunction with the combined treatments discussed here, 4–12 h postirradiation appears to be the optimal time for administration.

In this work, tumor oxygenation was not directly measured, although it is known that oxygenation levels in tumors are a critical factor in response to radiation. However, since perfusion and distribution volume was measured, it is probable that surrogate measures of tumor oxygenation were available, at least for the tumor as a whole. With that in mind, it might be hypothesized that the preservation of flow in the 8 h group at the early time points after irradiation indicated an overall increase in oxygenation in the tumor, compared to the 1 h group and a subsequent improvement in response to radiation.

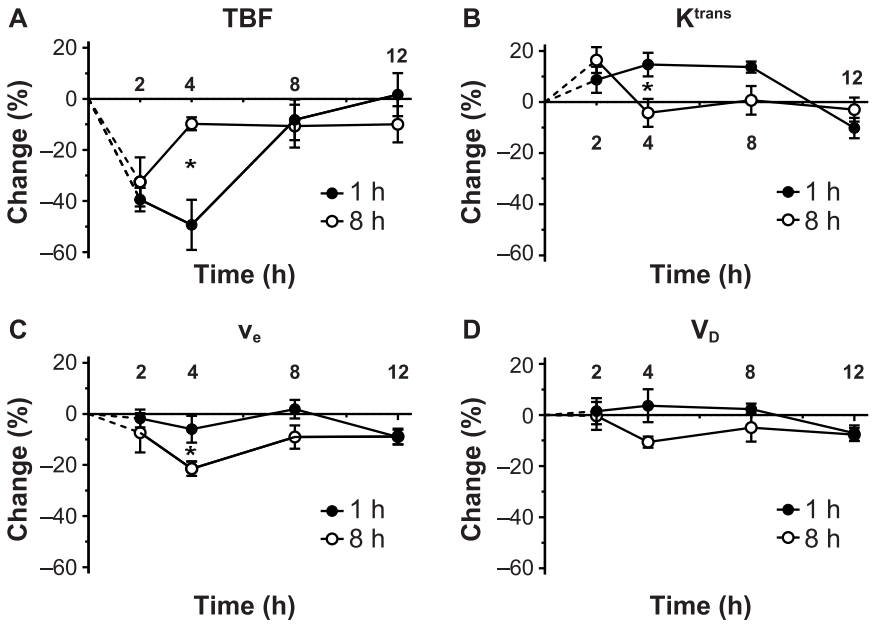

FIG. 5. Comparison of percentage changes between the 1 and 8 h groups for each parameter. Panels A–D: TBF, K^{trans}, V_D and v_e, respectively. Notably, there is great divergence in the vascular parameter values at the 4 h time point between the 1 and 8 h groups where the significant changes occur. TBF, K^{trans} and V_D values for the 1 and 8 h groups were significantly different at 4 h postirradiation ($P = 0.010$, 0.030 and 0.032, respectively), while v_e was not significantly different ($P = 0.071$). In contrast, ADC did not show any difference or particular pattern between 1 and 8 h groups (data not shown).

The findings from this study certainly have clinical implications. The drug Cilengitide entered phase III clinical trials [the CENTRIC EORTC 26071-22072 study (*43*)] for the treatment of gliomas; it was administered in addition to standard TMZ and radiotherapy. The result of this trial showed that the use of Cilengitide does not extend the OS in newly diagnosed GBM patients. However, it is worth noting that in the CENTRIC study, Cilengitide was administered without regard to optimal timing with radiotherapy. Thus, one of the reasons that Cilengitide may have shown no benefit in this trial may be that the critical matter of timing and the short-term effects of Cilengitide were not considered. Also, a lack of knowledge about the acute physiology of tumor response in the hours after combined treatments may have contributed to a missed opportunity to optimally combine these two treatments.

Exposure to radiation at the vascular normalization time window triggered by Cilengitide can lead to an amplification in the outcome of radiation exposure. In the 8 h group, our results support Cilengitide increasing the effectiveness of radiation injury through a change in the tumor environment and by increasing radiation-induced apoptosis and vascular normalization.

Acute changes in physiology may guide the optimization of other anti-angiogenic agents used in combination with radiation treatment. Recently, two placebo-controlled, randomized trials were conducted by the U.S. Radiation Therapy Oncology Group (RTOG) 0825 trial and the European Avastin in Glioblastoma (AVAglio) trial. These trials addressed the clinical benefit of adding bevacizumab to the best standard treatment for newly diagnosed GBM (radiotherapy and temozolomide). While the two trials were nearly identical in design, patient characteristics and the primary end points of progression-free survival and overall survival, the study results were contradictory. The U.S. study reported no benefit with the combined treatments (*44*), whereas the European study showed improved progression-free survival, maintenance of baseline quality of life and performance status, although no benefit to overall survival was reported (*45*). The reason for the difference remains unclear (*46*). The identification of a subset of patients that would benefit from the addition of bevacizumab was noted, and a call was made for the development of imaging markers and biomarkers that may be predictive of a response to bevacizumab in an individual patient (*46*). The MRI findings described herein may serve as an early predictor of tumor response based on the responsiveness of tumor vasculature and may have value for distinguishing those eventual responders from the nonresponders.

Furthermore, it has been recommended elsewhere (*3, 47, 48*) that the use of a combination of multi-pathway-targeted agents with conventional chemo-radiotherapy may improve the treatment outcome in GBMs. We believe that if treatments are combined in an informed manner, based on acute changes in tumor vascular parameters, they may offer a superior outcome; the sequence and delivery time between treatments may have a crucial impact on outcome and survival. Tracking the short-term changes in tumor physiology after a single treatment or combined treatments may help define the sequence and timing for an optimum

effect. The noninvasive MRI biomarkers used in this study can be useful tools to monitor the temporal vascular changes in tumors.

ACKNOWLEDGMENTS

Support for this work was provided by the National Institutes of Health, National Cancer Institute, for the project entitled, ''MRI Biomarkers of Response in Cerebral Tumors'' [grant no. R01 CA135329 (JRE)]. We appreciate and acknowledge the expert technical assistance provided by Jun Xu.

Received: December 14, 2015; accepted: October 3, 2016; published online: December 21, 2016

REFERENCES

1. Johnson DR, O'Neill BP. Glioblastoma survival in the United States before and during the temozolomide era. J Neurooncol 2012; 107:359–64.
2. Stupp R, Hegi ME, Mason WP, van den Bent MJ, Taphoorn MJ, Janzer RC, et al. Effects of radiotherapy with concomitant and adjuvant temozolomide versus radiotherapy alone on survival in glioblastoma in a randomised phase III study: 5-year analysis of the EORTC-NCIC trial. Lancet Oncol 2009; 10:459–66.
3. Palanichamy K, Chakravarti A. Combining drugs and radiotherapy: from the bench to the bedside. Curr Opin Neurol 2009; 22:625–32.
4. Mikkelsen T, Brodie C, Finniss S, Berens ME, Rennert JL, Nelson K, et al. Radiation sensitization of glioblastoma by Cilengitide has unanticipated schedule-dependency. Int J Cancer 2009; 124:2719–27.
5. Zhao D, Chang CH, Kim JG, Liu H, Mason RP. In vivo near-infrared spectroscopy and magnetic resonance imaging monitoring of tumor response to combretastatin A-4-phosphate correlated with therapeutic outcome. Int J Radiat Oncol Biol Phys 2011; 80:574–81.
6. Rao SS, Thompson C, Cheng J, Haimovitz-Friedman A, Powell SN, Fuks Z, et al. Axitinib sensitization of high single dose radiotherapy. Radiother Oncol 2014; 111(1):88–93.
7. Nagaraja TN, Aryal MP, Brown SL, Bagher-Ebadian H, Mikkelsen T, Yang JJ, et al. Cilengitide-induced temporal variations in transvascular transfer parameters of tumor vasculature in a rat glioma model: identifying potential MRI biomarkers of acute effects. PLoS One 2013; 8:e84493.
8. Brown SL, Nagaraja TN, Aryal MP, Panda S, Cabral G, Keenan KA, et al. MRI-tracked tumor vascular changes in the hours after single-fraction irradiation. Radiat Res 2015; 183:713–21.
9. Eisenhauer EA. Response evaluation: beyond RECIST. Ann Oncol 2007; 18 Suppl 9:ix29–32.
10. Eisenhauer EA, Therasse P, Bogaerts J, Schwartz LH, Sargent D, Ford R, et al. New response evaluation criteria in solid tumours: revised RECIST guideline (version 1.1). Eur J Cancer 2009; 45:228–47.
11. Wen PY, Macdonald DR, Reardon DA, Cloughesy TF, Sorensen AG, Galanis E, et al. Updated response assessment criteria for high-grade gliomas: response assessment in Neuro-Oncology Working Group. J Clin Oncol 2010; 28:1963–72.
12. Vogelbaum MA, Jost S, Aghi MK, Heimberger AB, Sampson JH, Wen PY, et al. Application of novel response/progression measures for surgically delivered therapies for gliomas: Response Assessment in Neuro-Oncology (RANO) Working Group. Neurosurgery 2012; 70:234–44.
13. Kurozumi K, Ichikawa T, Onishi M, Fujii K, Date I. Cilengitide treatment for malignant glioma: current status and future direction. Neurol Med Chir (Tokyo) 2012; 52:539–47.
14. Goel S, Fukumura D, Jain RK. Normalization of the tumor vasculature through oncogenic inhibition: An emerging paradigm in tumor biology. Proc Natl Acad Sci U S A 2012; 109:E1214.
15. Abdollahi A, Griggs DW, Zieher H, Roth A, Lipson KE, Saffrich R, et al. Inhibition of alpha(v)beta3 integrin survival signaling enhances antiangiogenic and antitumor effects of radiotherapy. Clin Cancer Res 2005; 11:6270–9.
16. Reardon DA, Nabors LB, Stupp R, Mikkelsen T. Cilengitide: an integrin-targeting arginine-glycine-aspartic acid peptide with promising activity for glioblastoma multiforme. Expert Opin Investig Drugs 2008; 17:1225–35.
17. Truman JP, Garcia-Barros M, Kaag M, Hambardzumyan D, Stancevic B, Chan M, et al. Endothelial membrane remodeling is obligate for anti-angiogenic radiosensitization during tumor radiosurgery. PLoS One 2010; 5.
18. Beal K, Abrey LE, Gutin PH. Antiangiogenic agents in the treatment of recurrent or newly diagnosed glioblastoma: analysis of single-agent and combined modality approaches. Radiat Oncol 2011; 6:2.
19. Lomonaco SL, Finniss S, Xiang C, Lee HK, Jiang W, Lemke N, et al. Cilengitide induces autophagy-mediated cell death in glioma cells. Neurooncol 2011; 13:857–65.
20. Ewing JR, Brown SL, Lu M, Panda S, Ding G, Knight RA, et al. Model selection in magnetic resonance imaging measurements of vascular permeability: Gadomer in a 9L model of rat cerebral tumor. J Cereb Blood Flow Metab 2006; 26:310–20.
21. Bagher-Ebadian H, Jain R, Nejad-Davarani SP, Mikkelsen T, Lu M, Jiang Q, et al. Model selection for DCE-T1 studies in glioblastoma. Magn Reson Med 2012; 68:241–51.
22. Ewing JR, Bagher-Ebadian H. Model selection in measures of vascular parameters using dynamic contrast-enhanced MRI: experimental and clinical applications. NMR Biomed 2013; 26:1028–41.
23. Patlak CS, Blasberg RG, Fenstermacher JD. Graphical evaluation of blood-to-brain transfer constants from multiple-time uptake data. J Cereb Blood Flow Metab 1983; 3:1–7.
24. Patlak CS, Blasberg RG. Graphical evaluation of blood-to-brain transfer constants from multiple-time uptake data. Generalizations. J Cereb Blood Flow Metab 1985; 5:584–90.
25. Logan J, Fowler JS, Volkow ND, Wolf AP, Dewey SL, Schlyer DJ, et al. Graphical analysis of reversible radioligand binding from time-activity measurements applied to [N-11C-methyl]-(-)-cocaine PET studies in human subjects. J Cereb Blood Flow Metab 1990; 10:740–7.
26. Logan J. Graphical analysis of PET data applied to reversible and irreversible tracers. Nucl Med Biol 2000; 27:661–70.
27. Ewing JR, Wei L, Knight RA, Pawa S, Nagaraja TN, Brusca T, et al. Direct comparison of local cerebral blood flow rates measured by MRI arterial spin-tagging and quantitative autoradiography in a rat model of experimental cerebral ischemia. J Cereb Blood Flow Metab 2003; 23:198–209.
28. Williams D, Detre J, Leigh J, Koretsky A. Magnetic Resonance imaging of perfusion using spin inversion of arterial water. Proc Natl Acad Sci U S A 1992; 89:212–6.
29. Aryal MP, Nagaraja TN, Brown SL, Lu M, Bagher-Ebadian H, Ding G, et al. Intratumor distribution and test-retest comparisons of physiological parameters quantified by dynamic contrast-enhanced MRI in rat U251 glioma. NMR Biomed 2014; 27:1230–8.
30. Aryal MP, Nagaraja TN, Keenan KA, Bagher-Ebadian H, Panda S, Brown SL, et al. Dynamic contrast enhanced MRI parameters and tumor cellularity in a rat model of cerebral glioma at 7 T. Magn Reson Med 2014; 71:2206–14.
31. Tofts PS, Brix G, Buckley DL, Evelhoch JL, Henderson E, Knopp MV, et al. Estimating kinetic parameters from dynamic contrast-enhanced T(1)-weighted MRI of a diffusable tracer: standardized quantities and symbols. J Magn Reson Imaging 1999; 10:223–32.
32. Bailar JC, Hoaglin DC. Medical uses of statistics: Hoboken, NJ: John Wiley & Sons; 2012.

33. Kim JH, Kim CK, Park BK, Park SY, Huh SJ, Kim B. Dynamic contrast-enhanced 3-T MR imaging in cervical cancer before and after concurrent chemoradiotherapy. Eur Radiol 2012; 22:2533–9.

34. Thompson G, Mills SJ, Coope DJ, O'Connor JP, Jackson A. Imaging biomarkers of angiogenesis and the microvascular environment in cerebral tumours. Br J Radiol 2011; 84 Spec No 2:S127–44.

35. Farrar CT, Kamoun WS, Ley CD, Kim YR, Catana C, Kwon SJ, et al. Sensitivity of MRI tumor biomarkers to VEGFR inhibitor therapy in an orthotopic mouse glioma model. PLoS One 2011; 6:e17228.

36. Winkler F, Kozin SV, Tong RT, Chae SS, Booth MF, Garkavtsev I, et al. Kinetics of vascular normalization by VEGFR2 blockade governs brain tumor response to radiation: role of oxygenation, angiopoietin-1, and matrix metalloproteinases. Cancer Cell 2004; 6:553–63.

37. Horsman MR, Nielsen T, Østergaard L, Overgaard J. Radiation administered as a large single dose or in a fractionated schedule: Role of the tumour vasculature as a target for influencing response. Acta Oncol 2006; 45:876–80.

38. Jain RK. Normalization of tumor vasculature: an emerging concept in antiangiogenic therapy. Science 2005; 307:58–62.

39. Scaringi C, Minniti G, Caporello P, Enrici RM. Integrin inhibitor Cilengitide for the treatment of glioblastoma: a brief overview of current clinical results. Anticancer Res 2012; 32:4213–23.

40. Jain RK. Normalizing tumor microenvironment to treat cancer: bench to bedside to biomarkers. J Clin Oncol 2013; 31:2205–18.

41. Sorensen AG, Emblem KE, Polaskova P, Jennings D, Kim H, Ancukiewicz M, et al. Increased survival of glioblastoma patients who respond to antiangiogenic therapy with elevated blood perfusion. Cancer Res 2012; 72:402–7.

42. Platonova A, Koltsova SV, Hamet P, Grygorczyk R, Orlov SN. Swelling rather than shrinkage precedes apoptosis in serum-deprived vascular smooth muscle cells. Apoptosis 2012; 17:429–38.

43. Stupp R, Hegi ME, Gorlia T, Erridge SC, Perry J, Hong YK, et al. Cilengitide combined with standard treatment for patients with newly diagnosed glioblastoma with methylated MGMT promoter (CENTRIC EORTC 26071-22072 study): a multicentre, randomised, open-label, phase 3 trial. Lancet Oncol 2014; 15:1100–8.

44. Gilbert MR, Dignam JJ, Armstrong TS, Wefel JS, Blumenthal DT, Vogelbaum MA, et al. A randomized trial of bevacizumab for newly diagnosed glioblastoma. N Engl J Med 2014; 370:699–708.

45. Chinot OL, Wick W, Mason W, Henriksson R, Saran F, Nishikawa R, et al. Bevacizumab plus radiotherapy-temozolomide for newly diagnosed glioblastoma. N Engl J Med 2014; 370:709–22.

46. Fine HA. Bevacizumab in glioblastoma–still much to learn. N Engl J Med 2014; 370:764–5.

47. Reardon DA, Cheresh D. Cilengitide: a prototypic integrin inhibitor for the treatment of glioblastoma and other malignancies. Genes Cancer 2011; 2:1159–65.

48. Scaringi C, Enrici RM, Minniti G. Combining molecular targeted agents with radiation therapy for malignant gliomas. Onco Targets Ther 2013; 6:1079–95.